Manuscript Draft: Aim3 Leaf Traits

Bolívar Aponte Rolón Mareli Sánchez Juliá A. Elizabeth Arnold
Sunshine A. Van Bael

2023-12-26

1 Abstract

2 Keywords:

endophytes, atta colombica, herbivory, calonectria, pathogen, foliar, fungal, symbionts

3 Introduction

Hypothesis 2 If FEF improves leaf defenses against plant pests, then generalist herbivores and pathogens will remove or damage less leaf tissue from plants with treated high FEF levels relative to those with low FEF loads.

Predictions.

Leaf-cutter ants will remove less plant material from leaves with higher FEF abundance and richness, but this result will be modulated by leaf traits related to defenses. Leaves with longer lifespans will be less attractive to leaf-cutter ants. Alternatively, low FEF diversity in those leaves may outweigh this selection factor. Leaves treated with high FEF levels will have a smaller area of pathogen damage compared to those treated with

low FEF levels. Endophyte-mediated defenses against pathogens will be most important in short-lived leaves since long-lived leaves are expected to rely more on constitutive defenses (e.g., leaf toughness).

4 Materials and Methods

4.1 Field

Growth and host plant inoculation seven tropical tree species was conducted at the greenhouses in the Gamboa Research Station, Smithsonian Tropical Research institute, Republic of Panama. The species, *Theobroma cacao*, *Dypterix* sp., *Lacmellea panamensis*, *Apeiba membranacea*, *Heisteria concinna*, *Chrysophyllum caimito*, and *Cordia alliodora* were chosen due to their variance in leaf traits (J.Wright unpublished data) and the availability of seeds in January- April 2019. Seeds of tree species were collected from the forest floor and grown in the greenhouse. Seedlings were kept in a chamber made out of PVC and clear plastic to prevent inoculation from spore fall inside the greenhouse. NEEDS INFORMATION ON THE SOIL MIXTURE AND AUTOCLAVING PROTOCOL. Seedlings reached a minimum of 4 true leaves before endophyte inoculation. Then 10 individual plants of each species were exposed to 10 nights of spore fall to achieve a high endophyte load (E+) and 10 homologous plants were kept inside the greenhouse plastic chamber to maintain a low endophyte load (*E*-) (Fig. ? MAKE A DIRAGRAM?). Plants exposed to spore fall were placed near (~10 m) the forest edge at dusk (~18:OO hours) and returned to the greenhouse at dawn (~07:00 hours) (**bittleston2011?**).

4.1.1 Leaf trait measurements

Three mature leaves were haphazardly collected from each of the individual plants in each treatment (E+, E-) within 7-10 days after inoculation treatment. Anthocyanin (ACI) content and leaf thickness (LT) were

measured while the leaf was still attached to the plant. We measured anthocyanin content with ACM-200plus (Opti-Sciences Inc. Hudson, New Hampshire, U.S.A.) on three haphazardly selected locations (working from the petiole out to the leaf tip) on the leaf surface of three haphazardly selected leaves for a total of nine measurements per plant (Tellez et al., 2022). The ACM-200 calculates an anthocyanin content index (ACI) value from the ratio of % transmittance at 931 nm/% transmittance at 525 nm (**opti-sciencesinc?**) . On compound leaves (i.e., *Dypterix* sp.) we measured at three different leaflets. Leaf thickness (µm) was measured with a Mitutoyo 7327 Micrometer Gauge (Mitutoyo, Takatsu-ku, Kawasaki, Japan) in sthe same manner as the anthocyanin measurements, taking care to avoid major and secondary veins. After anthocyanin and leaf thickness measurements were completed, we removed the leaves from their stems, placed them inside a plastic bag (i.e. Ziploc), place in an ice chest and moved them to the lab for further measurements. Leaf punch strength (LPS) was measured with an Imada DST-11a digital force gauge (Imada Inc., Northbrook, IL, United States) by conducting punch-and-die tests with a sharp-edged cylindrical steel punch (2.0 mm diameter) and a steel die with a sharp-edged aperture of small clearance (0.05 mm). The leaf punch measurements were taken by puncturing the leaf lamina at the base, mid-leaf and tip on both sides of the mid-vein, avoiding minor leaf veins when possible (Tellez et al., 2022). Once leaf toughness was measured, we used a 7 mm diameter punch hole to puncture disks for leaf mass per area (LMA) measurements. We collected one three disks per leaf (see Supplementary material for details). The disk punches dried at 60 °C for 48-72 hours. before being weighed.

4.1.2 Leaf tissue preparation for molecular work

The selected leaves were also used to profile endophyte community composition, abundance, and richness via amplicon sequencing (Illumina MiSeq). The leaf tissue remaining after the leaf trait measurements had the main vein and margins excised so that only the lamina remained. The lamina was haphazardly cut into 2 x 2 mm segments, enough to obtain a total of 16, and surface sterilized by sequential rinsing in 95% ethanol

(10 s), 0.5 NaOCl (2 mins) and 70% ethanol (2 mins), as per (Arnold et al., 2003; Higgins et al., 2014; Tellez et al., 2022). After, leaves were air-dried briefly under sterile conditions. Sixteen leaf segments per leaf, a total of forty-eight leaf segments per plant, were plated in 2% malt extract agar (MEA), sealed with Parafilm M (Bemis Company Inc., U.S.A.) and incubated at room temperature. The cultured leaf segments were used to estimate endophyte colonization of *E-* and *E+* leaves. The presence or absence of endophytic fungi in the leaf cuttings was assessed 7 days after plating. The remaining sterilized leaf lamina was preserved in sterile 15 mL tubes with ~ 10 mL CTAB solution (1 M Tris–HCl pH 8, 5 M NaCl, 0.5 M EDTA, and 20 g CTAB). Leaf tissue in CTAB solution was used for amplicon sequencing (described in detail below). All leaf tissue handling was performed in a biosafety cabinet with all surfaces sterilized by exposure to UV light for 30 minutes and cleaned sequentially in between samples with 95% ethanol, 0.5% NaOCl and 70% ethanol to prevent cross contamination.

4.2 Amplicon sequencing

Leaf tissue in CTAB solution was stored for 2 months at room temperature prior to being placed at -80 C for 3 months before extracting DNA. In preparation for DNA extraction, we decontaminated all instruments, materials, and surfaces with DNAway (Molecular BioProducts Inc., San Diego, CA, United States), 95% Ethanol, 0.5 % NaOCl, and 70 % Ethanol, and subsequently treated with UV light for 30 minutes in biosafety cabinet. We then transferred 0.2 – 0.3 g of leaf tissue into duplicate sterile 2mL tubes, resulting in 2 subsamples. Total genomic DNA from subsamples was extracted as described in U'Ren & Arnold (2017). In brief, we added two sterile 3.2 mm stainless steel beads to each tube and proceeded to lyophilize samples for 72 hours to fully remove CTAB content from tissue. After this period, we submerged the sample tubes in liquid nitrogen for 30s and proceeded to homogenize samples to a fine powder for 45 s in FastPrep-24 Tissue and Cell Homogenizer (MP Biomedicals, Solon, OH, USA). Afterwards, we repeated the decontamination procedure described before and used QIAGEN DNeasy 96 PowerPlant Pro-HTP Kit (U'Ren & Arnold, 2017)

(QIAGEN, Valencia, CA, USA). After all genomic DNA was extracted, we pooled the subsamples for each individual sample before amplification. We used sterile equipment and pipettes with aerosol-resistant tips with filters in all steps before amplification. We followed a two-step amplification approach previously described by Sarmiento et al. (2017) and U´Ren & Arnold (2017). We used primers for the fungal ITSrDNA region, ITS1f (5'-CTTGGTCATTTAGAGGAAGTAA-3') and ITS4 (5'-TCCTCCGCTTATTGATATGC-3') with modified universal consensus sequences CS1 and CS2 and 0–5 bp for phase-shifting. Every sample was amplified in two parallel reactions containing 1-2 µL of DNA template (U'Ren & Arnold, 2017; see also Tellez et al., 2022). We visualized PCR (PCR1) reactions with SYBR Green 1 (Invitrogen, Carlsbad, CA, USA) on 2% agarose gel (Oita et al., 2021). Based on the electrophoresis band intensity, we combined parallel PCR1 reactions and diluted 5 µL of amplicon product with molecular grade water to standardize to a concentration of 1:15 (Sarmiento et al., 2017 for details; Tellez et al., 2022). We included DNA extraction blanks and PCR1 negatives in this step. We used a separate set of sterile pipettes, tips, and equipment to reduce contamination. We used a designated PCR area to restrict contact with pre-PCR materials (Oita et al., 2021).

We used 1 µL of PCR1 product from samples and negative control for a second PCR (PCR2) with barcode adapters (IBEST Genomics Resource Core, Moscow, ID, USA). Each PCR2 reaction (total 15 µL) contained 1X Phusion Flash High Fidelity PCR Master Mix, 0.075 µM of barcoded primers (forward and reverse pooled at a concentration of 2 µM) and 0.24mg/mL of BSA following Sarmiento (2017) and U'Ren & Arnold (2017). Before final pooling for sequencing, we purified the amplicons using Agencourt AMPure XP Beads (Beckman Coulter Inc, Brea, CA USA) to a ratio of 1:1 following the manufacturer's instructions. The products were evaluated with Bio Analyzer 2100 (Agilent Technologies, Santa Clara, CA, USA) (Tellez et al., 2022). We quantified the samples through University of Arizona Genetics Core, and subsequently diluted them to the same concentration to prevent over representation of samples with higher concentration, see (CITATION). Amplicons were normalized to 1 ng/µL, then pooled 2 µL of each for sequencing. No contamination was

detected visually or by fluorometric analysis. To provide robust controls we combined 5 µL of each PCR1 negative and the DNA extraction blanks and sequenced them as samples. Ultimately, we combined samples into a single tube with 20 ng/µL of amplified DNA with barcoded adapters for sequencing on the Illumina MiSeq platform with Reagent Kit v3 (2 × 300 bp) following protocols from the IBEST Genomics Resource Core at the University of Idaho, USA. Again, we included the DNA extraction blanks and two PCR1 negatives and sequenced with samples. Sequencing yielded 3,778,081 total ITS1 reads.

4.2.1 Replication Statement (maybe goes before statistical analyses)

*In the Materials and Methods section (before the description of the data analyses), authors **MUST** state i) the scale at which they seek to make inferences (for example at the level of species, populations or experimental units); ii) the scale(s) at which their treatment or factor of interest is(are) applied; and iii) the number of replicates for each level of treatment or factor. We have provided a table template for including this information, which the editors will use to decide whether the authors' inferences are supported and should therefore be peer-reviewed. Manuscripts without this table will be returned to authors.*

4.2.2 Mock Communities

We processed and sequenced 12 mock communities following the methods described above. This allowed us to assess the quality of our NGS data set. We used two mock communities that consisted of PCR product from DNA extractions of 32 phylogenetically distinct fungi, representing lineages that are typically observed as endophytes: Ascomycota, Basidiomycota, Zygomycota and Chytridiomycota (Oita et al., 2021; see Daru et al., 2019 for details). In brief, we used six mock communities with equimolar concentrations of DNA from all 32 fungal taxa and another six mock communities with tiered concentrations of DNA from the same fungal taxa (Daru et al., 2019). Each mock community was sequenced five times (i.e., five replicates) (Oita

et al., 2021). The read abundance from the equimolar and tiered communities was positively associated with the expected read number (with replicates as a random factor: R2Adj = 0.87, P = XXXX, see Supplementary Material). Using mock communities allowed us to evaluate the sequencing effectiveness in communities with known composition and structure (Bowman & Arnold, 2021). Henceforth, we used read abundance as a relevant proxy for biological OTU abundance (U'Ren et al., 2019).

4.2.3 Bioinformatic analyses

We used VSEARCH (v2.14.1) for *de novo* chimera detection, dereplication and sequence alignment. VSEARCH is an open-source alternative to USEARCH that uses an optimal global aligner (full dynamic programming Needleman-Wunsch), resulting in more accurate alignments and sensitivity (Rognes et al., 2016). For mock communities and experimental samples, we used forward reads (ITS1) for downstream bioinformatics analyses due to their high quality, rather than reverse reads (ITS4). Following Sarmiento et al. (2017), we concatenated all reads in a single file and used FastQC reports to assess Phred scores above 30 and determine the adequate length of truncation. We processed 892,713 of sequence reads from mock communities and 3,778,081 from experimental samples. We truncated mock community and experimental sample reads to a length of 250 bp with command `fast_trunclen` and filtered them at a maximum expected error of 1.0 with command `fast_maxee`. We then clustered unique sequence zero radius OTUs (that is, zOTUs; analogous to amplicon sequence variants (Callahan et al., 2016)), by using commands `derep_fulllength` and `minseqlength` set at 2. Sequentially we denoised and removed chimeras from read sequences with commands `cluster_unoise`, and `uchime3_denovo`, respectively (see Supplementary YYY for details). Finally, we clustered zOTUs at a 95% sequence similarity with command `usearch_global` and option `id` set at 0.95. After which, 3,035,960 sequence reads from experimental samples remained.

Taxonomy was assigned with the Tree-Based Alignment Selector Toolkit [v2.2; Carbone et al. (2019)] by placing unknowns within the Pezizomycotina v2 reference tree (Carbone et al., 2017). ITS sequences were blasted against the UNITE database by the ribosomal database project (RDP) classifier. A total of 2147 OTUs hits were obtained and are composed of 68.6% Ascomycota, 26.8% Basidiomycota,<0.05% Chytridiomycota, <0.05% Glomeromycota, <0.05% Mortierellomycota, <0.05% Rozellomycota, 0.05% Kickxellomycota, and 4.2 % BLAST hit misses. Only OTUs representing Ascomycota were used for downstream statistical analyses since foliar endophyte communities in tropical trees are dominated by Ascomycota (Arnold & Lutzoni, 2007).

For each OTU identified, we removed laboratory contaminants from experimental samples by substracting the average read count found in control samples from the DNA extraction and PCR steps. Our analysis of mock communities allowed use to identify and remove false OTUs from experimental samples, those with fewer than 10 reads, and remove 0.1% of the read relative abundance across all samples (Oita et al., 2021). Removed reads represent the frequency of reads classified as contamination in the mock communities relative to the expected read count. Three experimental samples from *Theobroma cacao* (n=2) and *Apeiba membranacea* (n=1) were removed from all analyses due to incomplete entries. After pruning taxa with zero reads from experimental samples, we identified 260 OTUs found exclusively in control ($E-$) plants (n=78) and deemed them as artifacts resulting from the greenhouse conditions. Consequently, these were consistently eliminated from treatment ($E+$) plants across all species. We converted reads for each fungal OTU to proportions of total sequence abundance per sample to reduce differences in sampling effort, following previous studies (Weiss et al. (2017); McMurdie & Holmes (2014)). We then removed singletons and obtained an average of 2,464,558 sequence reads in 529 Ascomycota OTUs across 156 experimental samples of 7 tree species. All analyses post taxonomic assignment were performed in R [v. 4.3.2; R Core Team (2023)] using the `phyloseq` package (McMurdie & Holmes, 2013) and custom scripts (see Supplementary Material).

4.2.4 Ant-endophyte interaction assays

A fresh fourth leaf was used in ant assays. To assess leaf-cutter ant damage, we introduced one detached leaf per plant per treatment to an actively foraging leaf-cutter ant colony for a two-hour assay. We presented leaf-cutter ant colonies with a choice of an E+ or an E- leaf on one disposable plastic plate next to an active nest trail. Carefully, we collected and placed debris from the trail leading up to the plate to lure ants into the plate. We initiated the ant assay as soon as one ant entered the plate and explored the leaf contents (for ~ 10-20 seconds). Every five minutes we took a digital photo of the choice arena until about 75% of the leaf content of one of the leaves was consumed. We used the digital photo at time zero and at the end of trial to quantify the leaf area removed using ImageJ [v1.52r; Schneider et al. (2012)]. Ant recruitment was estimated by counting individuals in the choice arena throughout trial event.

4.2.5 Pathogen assays

For the pathogen assays, we introduced an agar plug inoculated with hyphae of *Calonectria* sp. ($P+$ treatment), and an agar plug without the pathogen ($P-$ control) to similarly aged/sized leaves within 10-14 days after endophyte inoculations (CITATION). Leaves with the $P+$ or $P-$ treatment were misted with sterile water two times a day (morning and afternoon) to maintain moisture. After four days, we removed the plugs and took digital photos to analyze leaf area damage using ImageJ [v1.52r; Schneider et al. (2012)].

4.2.6 Statistical Analyses

We explored how leaf functional traits and foliar fungal symbionts correlated to herbivory and pathogen damage on leaves. We present the analyses at the leaf and at the plant level. Leaf functional traits were measured and are presented in their raw form, at the leaf level, while FEF data was explored and is presented

at the plant level. In analyses where leaf functional traits and FEF are combined we used averages of the leaf functional traits.

Principal Component Analysis (PCA) was used to reduce dimensions among covariates and reveal underlying interactions that could influence fungal endophyte abundance, diversity and community composition in seedlings. The PCA was computed using the `prcomp` function in R statistical software (R Core Team, 2023). A complete PCA was computed with variables ACI, LT, LPS, and LMA (Fig. 2a). We then proceeded to compute a PCA with the data from leaves of plants used in the ant (n = 210) and pathogen assays (n = 192). To further explore the interactions of between herbivory and pathogen damage against ACI, LT, LPS and LMA we computed simple linear regressions (Fig. S6 - S7).

To test for H2, we used a general linear mixed model (GLM) with herbivory and pathogen damage percentage (logit transformed) as the response variable. To determine which fixed effects to include in the models we used the `vif` function in *R* to calculate the variance inflation factor for all explanatory variables (ACI, LT, LPS and LMA) (R Core Team, 2023). We then created a correlation matrix with `cor` function to assess correlations among covariates (SUPPLEMENTARY FIGURE?). We opted to maintain explanatory variables pertaining to physical barriers (LT, LPS and LMA) and exclude ACI from subsequent general linear models due to high collinearity with LPS (0.54) and LMA (0.73). Every variable kept exhibits some degree of collinearity and this is well recorded in the literature (CITE HERE).

5 Results

Seedlings exposed to forest spore fall, *E*+, had a significantly higher proportion of leaf segments colonized by fungal endophytes across all species (data from cultures, Fig. S1) Using our molecular data set we saw that seedlings with *E*+ treatment had a significantly higher fungal endophyte relative abundance (p = <0.05) for all tree species when compared to *E*- treatment with the exception of *C. cainito* and *H. concinna* (Fig. 1).

This reflects the successful inoculation of our treatment types. Despite these significant differences, there is a high degree of variability in endophyte relative abundance within each treatment type (Fig. 1).

For individuals of all tree species, we observed general differences in leaf functional traits summarized in Table 1. For LT we observed significant differences for *A. membranacea* , *Dypteryx* sp., and *L. panamensis* despite treatment type. Anthocyanins (ACI) were all leaf functional traits across all tree species. We did not see (CONTINUE HERE)

THE PARAGRAPH ABOVE NEEDS A LOT OF WORK. I NEED THE PLOTS FOR THIS TO WRITE ABOUT IT.

The PCA revealed how covariates (ACI, LT, LPS and LMA) interact. We plotted covariate data according to tree species groups on the PCA axes to show how the variance in the complete data set is explained by PC1 (60%) and PC2 (27%) (Fig. 2a). We observed that ACI, LPS and LMA loadings track along PC1 towards greater negative values, this indicative of correlation among these covariates (Fig. 2a). Covariates LT and LPS were orthogonal to each other in Fig. 2a, indicative of low correlation. We note distinct grouping of species along PC1 such as *C. alliodora* in direction of positive values of PC1 and *C. cainito* opposite. On PC1 we see distinct and tight clustering according to species in all groups except *H. concinna* and *A. membranacea* which overlap with various other species. We note that LT loading tracks towards negative values along PC2 (Fig.2a). Clear species groupings are detected, such as *Dypterix* sp. located towards positive values and *L. panamensis* towards negative values of the PC2 axis. We note a similar relationship between the covariates with respect to PC1 and PC2 in individual seedlings used for herbivory and pathogen damage trials (Fig. 2b-2c). The PCA of covariates from seedlings used in herbivory trials has a PC1 explaining 57.5% of the variance and a PC2 explaining 28% of the variance in the subset data (Fig. 2b). We saw an inversion of the LT loading in direction of positive values, as well as the main tree species clustered (i.e. *Dypteryx* sp. and *A. membranacea*) along PC2 (Fig. 2b) with respect to Fig. 2a. The PCA of covariates from seedling used in

pathogen damage trials has a PC1 explaining 64% of the variance and a PC2 explaining 25% of the variance in the subset data (Fig. 2c). We detected similar relationships among covariates and PC axes in the pathogen damage subset data (Fig. 2c) when compared to the complete data set (Fig. 2a).

Simple linear regressions of herbivory (%) against PC1 and PC2 reveal a statistically significant positive relationship (p = <0.001) (Fig. 3a and 3b). Even though we note large spread in the data (Fig. 3a and 3b), we see a statistically significant positive trend of herbivory plotted against PC1, were positive values represent greater values of ACI, LPS and LMA. Herbivory plotted against PC2 shows a statistically significant positive trend, were positive values represent greater LT (Fig. 3b). Percent pathogen damage plotted against PC1 reveal a statistically significant positive relationship (p = <0.001), were positive values represent greater values of ACI, LPS and LMA (Fig. 3c). We did not see a statistically significant relationship (p = 0.223) between pathogen damage and PC2 (Fig. 3d).

TALK ABOUT SIMPLE LINEAR REGRESSIONS OF SUPPLEMENTARY FIGURES?

6 Discussion

7 References

Arnold, A. E., & Lutzoni, F. (2007). Diversity and host range of foliar fungal endophytes: Are tropical leaves biodiversity hotspots? *Ecology*, *88*(3), 541–549. https://doi.org/10.1890/05-1459

Arnold, A. E., Mejía, L. C., Kyllo, D., Rojas, E. I., Maynard, Z., Robbins, N., & Herre, E. A. (2003). Fungal endophytes limit pathogen damage in a tropical tree. *Proceedings of the National Academy of Sciences*, *100*(26), 15649–15654.

Bowman, E. A., & Arnold, A. E. (2021). Drivers and implications of distance decay differ for ectomycorrhizal and foliar endophytic fungi across an anciently fragmented landscape. *The ISME Journal*, *15*(12),

3437–3454. https://doi.org/10.1038/s41396-021-01006-9

Callahan, B. J., McMurdie, P. J., Rosen, M. J., Han, A. W., Johnson, A. J. A., & Holmes, S. P. (2016). DADA2: High-resolution sample inference from Illumina amplicon data. *Nature Methods*, *13*(7), 581–583. https://doi.org/10.1038/nmeth.3869

Carbone, I., White, J. B., Miadlikowska, J., Arnold, A. E., Miller, M. A., Kauff, F., U'Ren, J. M., May, G., & Lutzoni, F. (2017). T-BAS: Tree-Based Alignment Selector toolkit for phylogenetic-based placement, alignment downloads and metadata visualization: An example with the Pezizomycotina tree of life. *Bioinformatics*, *33*(8), 1160–1168. https://doi.org/10.1093/bioinformatics/btw808

Carbone, I., White, J. B., Miadlikowska, J., Arnold, A. E., Miller, M. A., Magain, N., U'Ren, J. M., & Lutzoni, F. (2019). T-BAS Version 2.1: Tree-Based Alignment Selector Toolkit for Evolutionary Placement of DNA Sequences and Viewing Alignments and Specimen Metadata on Curated and Custom Trees. *Microbiology Resource Announcements*, *8*(29), e00328–19. https://doi.org/10.1128/MRA.00328-19

Daru, B. H., Bowman, E. A., Pfister, D. H., & Arnold, A. E. (2019). A novel proof of concept for capturing the diversity of endophytic fungi preserved in herbarium specimens. *Philosophical Transactions of the Royal Society B: Biological Sciences*, *374*(1763), 20170395. https://doi.org/10.1098/rstb.2017.0395

Higgins, K. L., Arnold, A. E., Coley, P. D., & Kursar, T. A. (2014). Communities of fungal endophytes in tropical forest grasses: Highly diverse host- and habitat generalists characterized by strong spatial structure. *Fungal Ecology*, *8*(1), 1–11. https://doi.org/10.1016/j.funeco.2013.12.005

McMurdie, P. J., & Holmes, S. (2013). Phyloseq: An R Package for Reproducible Interactive Analysis and Graphics of Microbiome Census Data. *PLoS ONE*, *8*(4), e61217. https://doi.org/10.1371/journal.pone.0061217

McMurdie, P. J., & Holmes, S. (2014). Waste Not, Want Not: Why Rarefying Microbiome Data Is Inadmissible. *PLoS Computational Biology*, *10*(4), e1003531. https://doi.org/10.1371/journal.pcbi.1003531

Oita, S., Ibáñez, A., Lutzoni, F., Miadlikowska, J., Geml, J., Lewis, L. A., Hom, E. F. Y., Carbone, I., U'Ren, J.

M., & Arnold, A. E. (2021). Climate and seasonality drive the richness and composition of tropical fungal endophytes at a landscape scale. *Communications Biology*, *4*(1), 313. https://doi.org/10.1038/s42003-021-01826-7

R Core Team. (2023). *R: A Language and Environment for Statistical Computing* [Computer software]. R Foundation for Statistical Computing. https://www.R-project.org/

Rognes, T., Flouri, T., Nichols, B., Quince, C., & Mahé, F. (2016). VSEARCH: A versatile open source tool for metagenomics. *PeerJ*, *4*, e2584. https://doi.org/10.7717/peerj.2584

Sarmiento, C., Zalamea, P. C., Dalling, J. W., Davis, A. S., Simon, S. M., U'Ren, J. M., & Arnold, A. E. (2017). Soilborne fungi have host affinity and host-specific effects on seed germination and survival in a lowland tropical forest. *Proceedings of the National Academy of Sciences of the United States of America*, *114*(43), 11458–11463. https://doi.org/10.1073/pnas.1706324114

Schneider, C. A., Rasband, W. S., & Eliceiri, K. W. (2012). NIH Image to ImageJ: 25 years of image analysis. *Nature Methods*, *9*(7), 671–675. https://doi.org/10.1038/nmeth.2089

Tellez, P. H., Arnold, A. E., Leo, A. B., Kitajima, K., & Van Bael, S. A. (2022). Traits along the leaf economics spectrum are associated with communities of foliar endophytic symbionts. *Frontiers in Microbiology*, *13*, 927780. https://doi.org/10.3389/fmicb.2022.927780

Tellez, P. H., Rojas, E., & Van Bael, S. (2016). Red coloration in young tropical leaves associated with reduced fungal pathogen damage. *Biotropica*, *48*(2), 150–153. https://doi.org/10.1111/btp.12303

U'Ren, J. M., & Arnold, A. E. (2017). 96 well DNA Extraction Protocol for Plant and Lichen Tissue Stored in CTAB. *Protocols.io*, 1–5.

U'Ren, J. M., Lutzoni, F., Miadlikowska, J., Zimmerman, N. B., Carbone, I., May, G., & Arnold, A. E. (2019). Host availability drives distributions of fungal endophytes in the imperilled boreal realm. *Nature Ecology & Evolution*, *3*(10), 1430–1437. https://doi.org/10.1038/s41559-019-0975-2

Weiss, S., Xu, Z. Z., Peddada, S., Amir, A., Bittinger, K., Gonzalez, A., Lozupone, C., Zaneveld, J. R.,

Vázquez-Baeza, Y., Birmingham, A., Hyde, E. R., & Knight, R. (2017). Normalization and microbial differential abundance strategies depend upon data characteristics. *Microbiome*, *5*(1), 27. https://doi.org/10.1186/s40168-017-0237-y

8 Figures

8.1 Figure 1

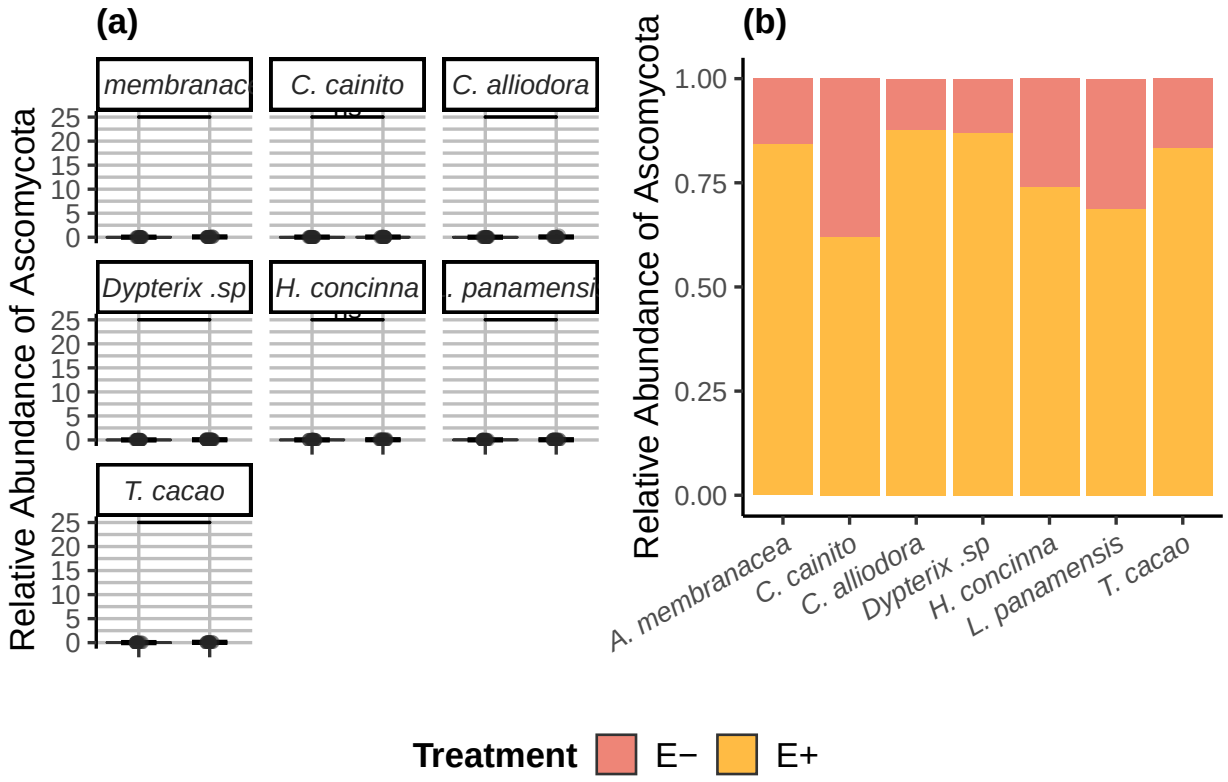

Figure 1: Relative abundance (RA) of Ascomycota OTUs of seven tree species used in the study. (a) Violin plots show individuals' RA and and its distribution by species. The horizontal line within the violins represent the mean RA per species. (b) The RA of OTU's by treatment withing each tree species. Pink filled violin plots represent low endophyte (*E*-) treatment and yellow filled violins represent high endophyte (*E*+) treatment. Relative abundance is the percentage of endophyte colonization within individuals of the same species. Significance levels are represented by asterisks [p = 0.05 (*), p = 0.01 (*), *and* p* = 0.001 (***)].

8.2 Figure 2

8.3 Figure 3

8.4 Figure 4

Linear mixed effects models for predicting leaf herbivory and pathogenicity

	logit herbivory			logit pathogenicity		
Predictors	Estimates	CI	p	Estimates	CI	p
(Intercept)	-0.26	-2.31 – 1.80	0.806	-3.42		

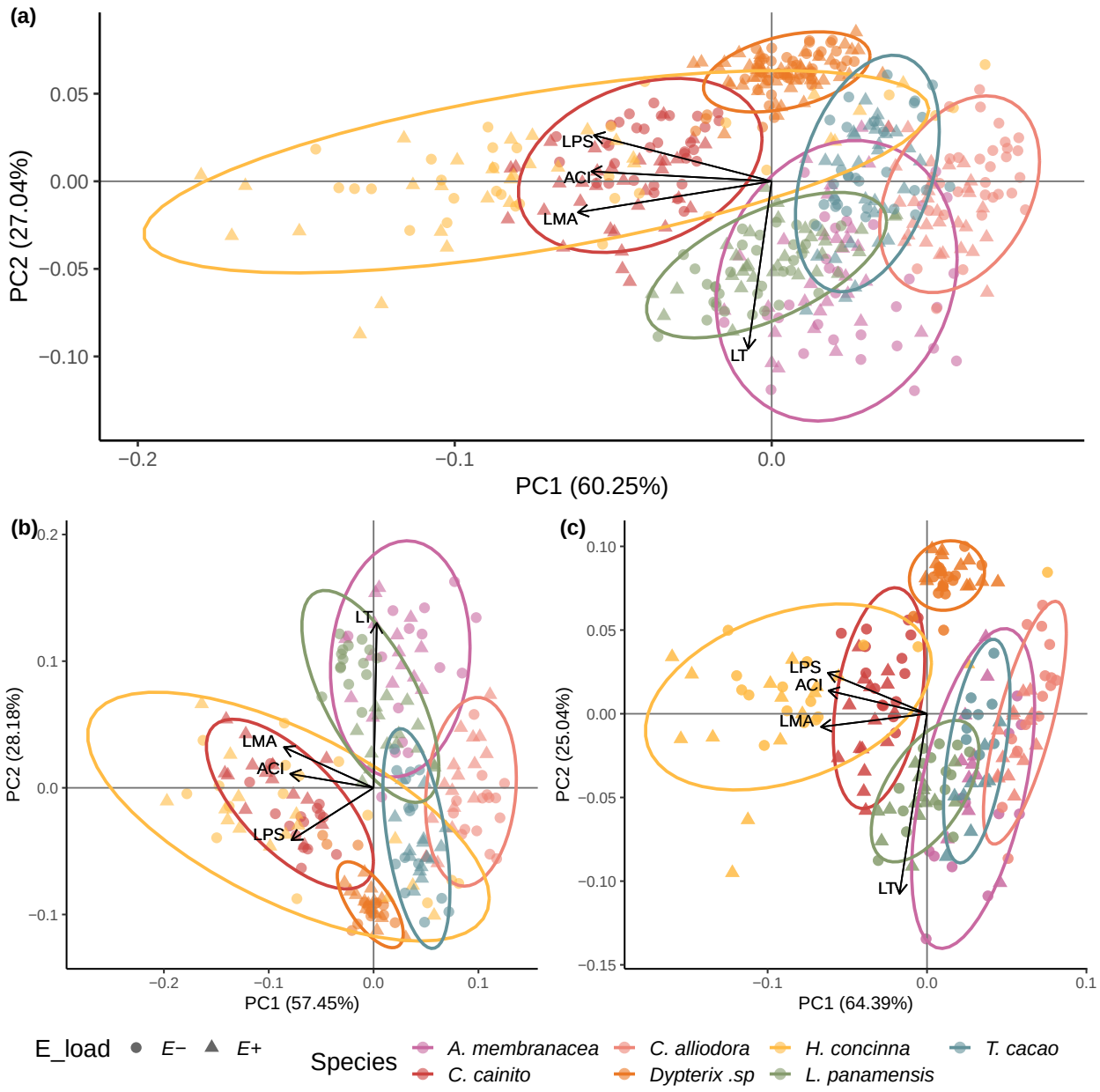

Figure 2: Leaf functional traits are conserved within tree species regardles of endophyte load treatment. (a) Principal Component Analysis (PCA) of leaf functional traits from all tree species separated by *E*- and *E*+ treatment. (b) PCA of leaf functional traits of plants solely used in ant herbivory assays. (c) PCA leaf functional traits of plants used solely in pathogen damage assays. Colors represent individual species. Circle and triangles represent los (*E*-) and high (*E*+) endophyte treatments, respectively. Colored ellipses correspond to tree species and represent 95% confidence intervals.

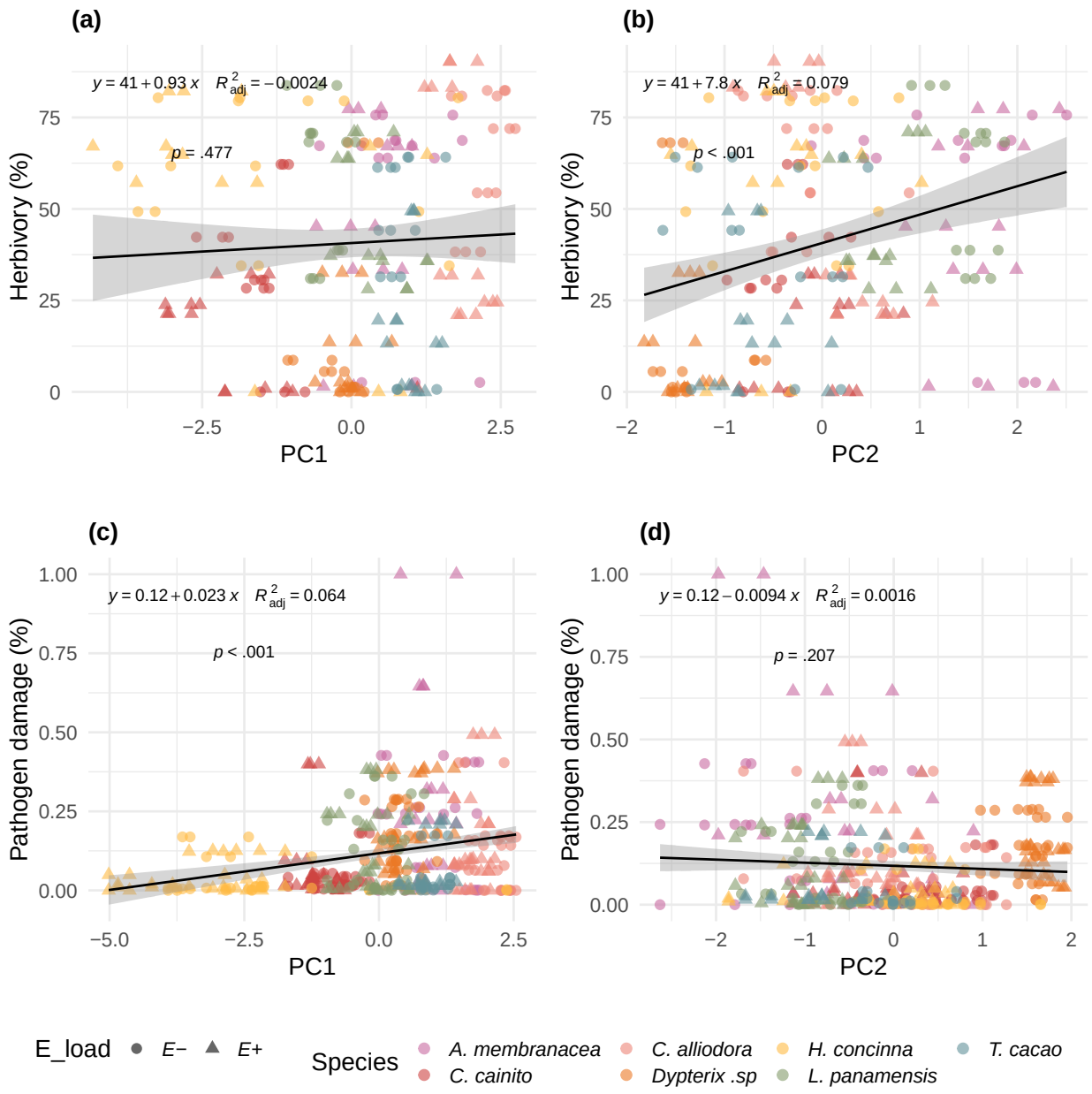

Figure 3: Simple linear regressions of herbivory and pathogen damage on PC1 and PC2 axes from PCAs of leaf traits for ant herbivory and pathogen damage assays. Linear regression of a) percent herbivory damage and PC1 axis (R^2-adjusted= -0.0024, p = 0.447); b) percent herbivory damage and PC2 axis (R^2-adjusted = 0.079, p = <0.001); c) percent pathogen damage and PC1 axis (R^2-adjusted = 0.064, p = <0.001); and d) percent pathogen damage and PC2 axis (R^2-adjusted = 0.0016, p = 0.207). Colors represent individual species. Circle and triangles represent *E*- and *E*+ treatments, respectively.

-4.40 – -2.43

<0.001

Thickness

-0.01

-0.02 – -0.00

0.013

0.00

-0.00 – 0.01

0.097

LMA

1741.22

768.82 – 2713.62

0.001

171.65

-181.40 – 524.70

0.340

E load [E+]

-0.78

-1.11 – -0.45

<0.001

Random Effects

σ^2

3.34

2.16

τ_{00}

1.93 $_{Species}$

0.80 $_{Treatment}$

0.02 $_{E\_load}$

0.96 $_{Species}$

ICC

0.37

N

7 $_{Species}$

2 $_{Treatment}$

369 2 E_load

370

371 7 Species

372 Observations

373 210

374 382

375 Marginal R^2 / Conditional R^2

376 0.089 / 0.423

377 0.011 / NA

378 AIC

379 745.559

380 1012.259

381 **8.5 Table 1**

Table 1: Summary statistics f

	A. membranacea, n = 83[1]	***C. alliodora, n = 100[1]***	***C. cainito, n = 150[1]***
Treatment			
E-	47	54	75

	A. membranacea, n = 83[1]	*C. alliodora, n = 100*[1]	*C. cainito, n = 150*[1]
E+	36	46	75
Anthocyanins (ACI)	5.35 ± 1.06	3.47 ± 0.43	8.21 ± 1.41
Leaf Thickness (LT) (μm)	270 ± 45	207 ± 37	205 ± 30
Leaf Punch Strength (LPS) (N mm/-1)	0.22 ± 0.05	0.21 ± 0.05	0.53 ± 0.09
Leaf Mass per Area (LMA) (mg)	0.0011 ± 0.0002	0.0007 ± 0.0001	0.0015 ± 0.0002